INTERNATIONAL JOURNAL OF CLIMATOLOGY
Int. J. Climatol. **20**: 853–863 (2000)

NORTH ATLANTIC INFLUENCE ON TIGRIS–EUPHRATES STREAMFLOW

HEIDI M. CULLEN* and PETER B. deMENOCAL
Department of Earth and Environmental Sciences, Lamont–Doherty Earth Observatory of Columbia University, 61 Route 9W, Palisades, NY 10964, USA

Received 11 December 1998
Revised 7 September 1999
Accepted 9 September 1999

ABSTRACT

Changes in streamflow of the Tigris and the Euphrates Rivers are shown to be associated with the North Atlantic Oscillation (NAO), a large-scale mode of natural climate variability which governs the path of Atlantic mid-latitude storm tracks and precipitation in the eastern Mediterranean. Composite indices of Turkish winter (December–March, DJFM) temperature and precipitation are developed which capture the interannual–decadal climate variability for the Tigris–Euphrates headwater region, a significant source of freshwater for Turkey, Syria and Iraq. These indices are significantly correlated with the NAO, with 27% of the variance in precipitation accounted for by this natural mechanism. As evidenced by the recent widespread drought events of 1984, 1989 and 1990, the Tigris–Euphrates streamflow also exhibits significant, $\sim \pm 40\%$ variability, associated with extrema. Copyright © 2000 Royal Meteorological Society.

KEY WORDS: Turkey; interannual–decadal variability; temperature; precipitation; streamflow

1. INTRODUCTION

With the regional population increasing by 3.5% each year and irrigation practices consuming at least 80% of the available supply, water is a key variable affecting public health and political stability of the Middle East (Figure 1). As a result, the Middle East is extremely vulnerable to any, either natural or anthropogenic, reductions in available surface and ground water. Much of the current focus in Middle Eastern water policy has been the environmental and socio-economic impacts associated with increased damming along the Tigris–Euphrates River system. These anthropogenic changes have escalated trans-boundary water disputes, threatening the security of the region and arousing international concern (McCaffrey, 1993; Shapland, 1997; Kinzer, 1999). In this paper, it is demonstrated that much of the observed interannual–decadal variability in Middle Eastern climate and Tigris–Euphrates streamflow is physically linked to a well-known, natural mode of climate variabilty—the North Atlantic Oscillation (NAO) (Hurrell, 1995). The NAO, like the El Niño–Southern Oscillation (ENSO), is one of the large-scale modes of climate variability in the Northern Hemisphere (NH). It defines a large-scale meridional oscillation of atmospheric mass between the centre of subtropical high surface pressure located near the Azores and the subpolar low surface pressure near Iceland. Synchronous strengthening (positive NAO state) and weakening (negative NAO state) have been shown to result in distinct, dipole-like climate change patterns between western Greenland/Mediterranean and northern Europe/northeast US/Scandinavia (Walker, 1924; Walker and Bliss, 1932; van Loon and Rogers, 1978; Rogers and van Loon, 1979).

The primary focus of this study is to investigate the regional extent of the NAO in the Eastern Mediterranean sector, quantify the effects of these linkages in terms of measured environmental parameters (i.e. temperature and precipitation), and finally focus on the far-field impacts of the NAO in

* Correspondence to: Department of Earth and Environmental Sciences, Lamont–Doherty Earth Observatory of Columbia University, 61 Route 9W, Palisades, NY 10964, USA. Tel.: +1 914 365 8571; fax: +1 914 365 8157; e-mail: cullen@ldeo.columbia.edu

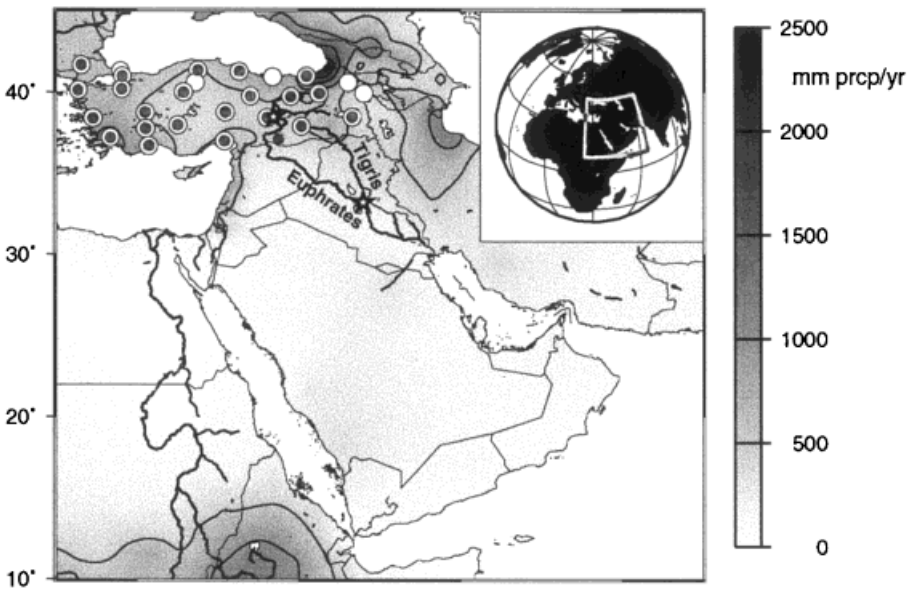

Figure 1. Middle East precipitation with selected Turkish temperature (23 small dark circles) and precipitation stations (27 large white circles); stations with less than 30 years of data or any incomplete DJFM series were omitted (Baker *et al*., 1995). Tigris and Euphrates River streamflow measurement stations in Keban, Turkey and Baghdad, Iraq are depicted with star symbols (Vorosmarty *et al*., 1996)

terms of Turkish temperature, precipitation and Tigris–Euphrates streamflow. This paper intends to explore the spatial extent of the NAO beyond the maritime North Atlantic sector and into the Middle East, a region commonly neglected from North Atlantic studies because of its proximity to the monsoonal region and its relatively sparse data coverage.

2. TURKEY: HOME TO THE TIGRIS–EUPHRATES HEADWATERS

Most of the Middle East has impoverished surface and groundwater resources owing to the subtropical predominance of evaporation over precipitation. One notable exception is Turkey, which has abundant excess precipitation primarily because of its orographic capture of winter rainfall from eastward propagating mid-latitude cyclones generated in the North Atlantic Ocean and the eastern Mediterranean Sea (Turkes, 1996a). Consequently, the Taurus Mountains and the Anatolian Highlands of eastern Turkey are the headwater regions for the Tigris and Euphrates Rivers (Figure 1), whose waters are shared primarily between Turkey and downstream riparians Syria and Iraq.

2.1. Spatio–temporal variations of temperature and precipitation in Turkey

Turkey is typically classified as having a Mediterranean macro-climate, which is defined by hot, dry summers and cool, wet winters resulting from the seasonal alternation of maritime subpolar and subtropical air masses (Henderson-Sellers et al., 1992). The main geographical controls on precipitation variability in Turkey are (i) the continental seas (Mediterranean, Black and Caspian Seas), which provide natural passages for frontal cyclones, and (ii) a west–east-oriented mountain range where the forced orographic ascent of air masses promotes heavy rainfall along windward slopes and loss of moisture content resulting from adiabatic 'drying' upon descent along the leeward side (Turkes, 1996b).

Home to the headwater region of both the Tigris and the Euphrates Rivers, runoff from the Taurus mountains of Turkey (Figure 1) supplies water to two-thirds of the Arabic-speaking population of the Middle East. Conservative estimates state that 88% of the water in the Euphrates River is derived from

precipitation falling in Turkey, with the remaining 12% coming from underground springs in Syria. Kolars and Mitchell (1991), however, believe that much of the water in these springs is Turkish in origin, and thereby calculate that 98% of Euphrates' streamflow originates in the Turkish headwater region. The Tigris receives almost 60% of its water below Baghdad, making it less sensitive but still linked to variations in Turkish precipitation.

The spatial distribution of precipitation over Turkey ranges from more than 2000 mm/year along the eastern coast of the Black Sea to 350 mm/year in the semi-arid central Anatolia region, with an average of 650 mm/year (Figure 1). In general, mean annual rainfall totals decrease from coastal belts to the interior, with a steep gradient over the Northern Anatolian and Taurus Mountain ranges. Rainfall decreases as it passes over the Taurus mountains because of rainshadow and subsidence, marking the point of entrance into Turkey's arid and semi-arid regions located in (i) the central Anatolia region and (ii) the southeastern Anatolia region. Local effects account for the large spatial variability observed in Turkish precipitation and introduce interstation variability.

Summer rainfall accounts for 10% of the annual mean, while autumn rainfall accounts for an additional 23% (Turkes, 1996b). The remaining 67% of countrywide annual rainfall occurs during winter (December–February, DJF) and spring (March–May, MAM), when the eastern Mediterranean basin, the Balkans and Turkey are influenced by eastward propagating mid-latitude and Mediterranean depressions (Turkes, 1996b).

2.2. Origin and genesis of cyclones

Both the Atlantic Ocean and the Mediterranean Sea are the primary source regions for the formation of winter (December–March, DJFM) precipitation-laden mid-latitude cyclones (Turkes, 1996b). These migratory low pressure systems have four primary cyclonic centres near to Crete, Cyprus, southern Italy and the Gulf of Genoa. Secondary centres are also found over the Black and the Caspian Seas because of their relatively warm sea surface temperatures (Alpert *et al.*, 1990). Satellite studies have shown that cyclones tend to follow the northern part of the Mediterranean Sea and then move onto land along one of three routes: (i) between the Balkan and the Turkish mountains; (ii) between the Swiss and the Dinarc Alps; and (iii) between the Turkish and the Syria/Lebanon mountains (Alpert *et al.*, 1990). Orographic ascent of the Atlantic maritime polar and Mediterranean air masses leads to heavy rainfall along the windward slopes of the Northern Anatolian and the Taurus Mountains. These two centres are the principal precipitation control for the region and determine the abundance and intensity of rainfall draining into the Tigris–Euphrates river system (Turkes, 1996b). In the following section, the relationship between these secondary cyclones and the NAO will be further described.

3. THE NORTH ATLANTIC OSCILLATION (NAO)

Originally described in the diaries of the missionary Saabye (1942) as a see-saw in temperature between Greenland and Denmark, the NAO was later defined by Walker as a meridional alternation of atmospheric mass (Walker, 1924; Walker and Bliss, 1932). Accounting for greater than one-third of the total variance of the sea level pressure (SLP) field over the North Atlantic, the NAO is most pronounced during the winter months (DJFM) because of an increased sea–air temperature contrast (Barnston and Livezey, 1987).

Because the signature of the NAO is strongly regional, a simple NAO index was defined as the difference between the normalized mean winter SLP anomalies at locations representative of the relative strengths of the Azores High (AH) and the Icelandic Low (IL). The first NAO_{SLP} index was defined by Walker and Bliss (1932) and simplified by Rogers (1984), who constructed an NAO_{SLP} index starting in 1894, using SLP anomalies from Ponta Delgados, Azores and Akuyreyri, Iceland. Hurrell (1995) selected Lisbon, Portugal and Stykkisholmur, Iceland in order to extend the record for another 30 years (Plate 1(a)). A positive NAO_{SLP} index implies more meridional storm tracks while a negative NAO_{SLP} index

implies more zonal storm tracks, which ultimately penetrate into the Mediterranean Sea (Alpert *et al.*, 1990), thereby remotely linking the Middle East to the North Atlantic. Investigation of the power spectrum of the NAO_{SLP} index for the past 130 winters (1864–1995) reveals a somewhat red spectrum with an indication of enhanced energy in the interannual (2–3 year) and decadal (6–10 year) frequency bands (Hurrell and Van Loon, 1997).

Hurrell (1995) investigated the relationship between variations in the NAO_{SLP} index and the decadal trends in NH temperature and precipitation, successfully demonstrating the existence of a climate dipole. Coherent, large-scale changes in the NAO since 1981 were linked to recent dry conditions over western Greenland and the Mediterranean, and wetter and warmer than normal conditions in northern Europe, the northeast US and parts of Scandinavia (Hurrell, 1995, 1996; Hurrell and Van Loon, 1997). Using multivariate linear regression to quantify temperature variability associated with the NAO, it was shown that the NAO accounts for 31% of NH interannual variance (Hurrell, 1996). Moreover, the NAO accounts linearly for 0.15°C of the 0.29°C NH extratropical temperature increase for the period 1981–1994, with respect to the 1935–1994 mean. Lamb and Peppler (1987) provided the first focused regional investigation of NAO teleconnections. They successfully linked decreased Moroccan rainfall to a positive state of the NAO, after receiving an invitation from the Moroccan Government, who at that time was concerned about the severe and persistent drought of 1979–1984.

Of particular relevance to the present study is the effect of NAO-related changes in mean atmospheric circulation on the strength and direction of precipitation-laden mid-latitude cyclones. A positive (negative) NAO refers to an intensified (weakened) poleward pressure gradient resulting from a synchronous strengthening (weakening) of the AH and deepening (shallowing) of the IL of the order of 15 mb (Hurrell, 1995). Resultant changes in mean circulation show meridionally (zonally) oriented westerlies moving onto Europe, increased (decreased) moisture transport, and a winter of higher (lower) than average precipitation in northern Europe, the northeast US and Scandinavia, and lower (higher) than average precipitation in western Greenland and the Mediterranean. The NAO is the dominant mode of interannual–decadal climate variability for the Atlantic sector, accounting for 20–60% of the variance over the last 150 years (Hurrell, 1995). It is these mid-latitude cyclones, associated with a negative state of the NAO, which migrate into the Mediterranean and generate secondary centres of precipitation-laden low pressure systems, thereby extending the spatial extent of the NAO dipole.

3.1. The Tigris–Euphrates river system

The Euphrates River, the longest in southwest Asia (2700 km), is formed by two tributaries: the Kara Su (elevation 2744 m) north of Erzurum and the Murat (elevation 3135 m) north of Lake Van (Figure 1). These two tributaries, along with the Balikh and the Khabur tributaries which join further downstream, drain the heavy winter/spring precipitation in the form of runoff from the southeastern Taurus Mountains (Gleick, 1993). Of the 509 billion cubic meters (BCM) of rainfall/year received by Turkey, 38% is in the form of surface runoff to the Tigris–Euphrates river system(Hillel, 1994).

The Tigris River, the second longest river in southwest Asia (1840 km), originates in eastern Turkey near Lake Hazar (elevation 1150 m) and flows southeast to the Turkish city of Cizre, where it forms the border with Syria before flowing into Iraq. Several tributaries contribute to the Tigris, including the Greater Zab, the Lesser Zab, the Adhaim and the Diyala. The Tigris and Euphrates converge near the Iraqi city of Qurna, and continue as the Shatt-al-Arab before draining into the Persian Gulf (Kolars and Mitchell, 1991).

The rivers have two primary flooding periods. November–March (NDJFM) constitutes the first rise and is mostly because of surface runoff from the NDJFM rainfall. The second rise, during April and May, results from snowmelt and generates 50% of the annual runoff (Kolars and Mitchell, 1991).

Annual streamflow volumes of the Tigris–Euphrates river system exhibited nearly sixfold variability during the period 1929–1972, before large-scale damming occurred, when records for this now tightly guarded variable were still available. Mean annual Euphrates streamflow is $\sim$32.5 BCM, of which $\sim$30 BCM arises from within Turkey. The historical minimum of Euphrates streamflow is 10.7 BCM

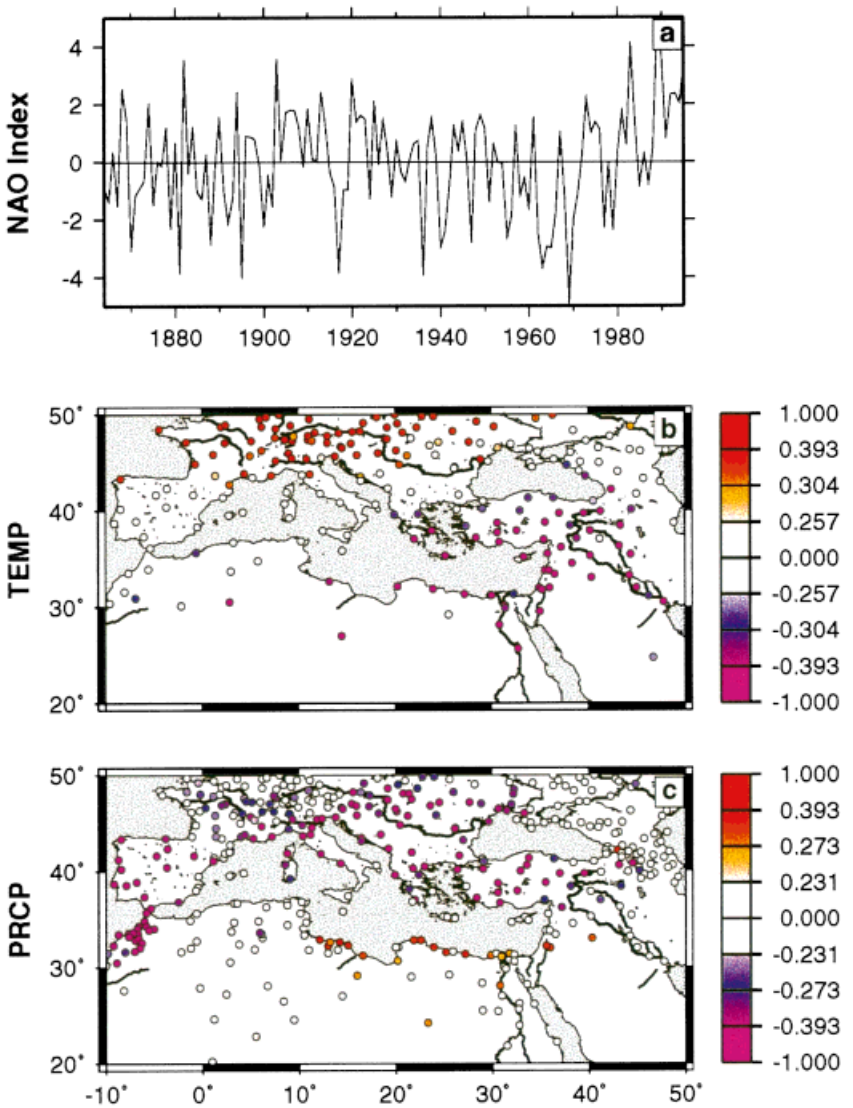

Plate 1. (a) The North Atlantic Oscillation sea level pressure index (NAO_{SLP}, 1864–1995) defined by Hurrell (1995); (b) spatial correlation between the NAO_{SLP} index and mean winter (DJFM) station temperature; and (c) spatial correlation between the NAO_{SLP} index and mean winter station precipitation

(1929–1930), whereas the maximum is 63.4 BCM (1968–1969) (Kolars and Mitchell, 1991). Mean annual Tigris streamflow at Cizre is ~ 19.7 BCM, with 29.5 BCM added by Iraqi tributaries Shapland (1997).

Secondary cyclogenesis in the Eastern Mediterranean provides a physical link between the Middle East and the NAO, and assigns the North Atlantic the role of primary provider of precipitation to the Middle East. Further quantifying of this far-field link will be accomplished by: (i) expressing the climate signature of the NAO in the Eastern Mediterranean by means of spatial correlation analysis; (ii) constructing a spatially averaged Turkish temperature and precipitation index; and (iii) quantifying the impact of variations in the NAO on Turkish temperature, precipitation and Euphrates River streamflow.

4. DATA AND METHODOLOGY

4.1. Data

The data used in this study consist of National Climatic Data Center (NCDC) Global Climate Perspectives System (GCPS) global monthly temperature and precipitation station data containing 6039 temperature and 7475 precipitation stations worldwide and extending from 1700 to 1995 (Baker *et al.*, 1995). The domain used in this study was 20°N–50°N, 10°W–50°E and consisted of 770 temperature and 591 precipitation stations extending from the Iberian Peninsula to the Middle East. The NAO_{SLP} index (Plate 1(a)) is the normalized winter SLP difference between Lisbon, Portugal and Stykkisholmur, Iceland, extending from 1864 to 1995, as constructed by Hurrell (1995).

The streamflow records used in this study, measured by tide-gauge (m^3/s), were obtained through UNESCO. Euphrates streamflow was measured at Keban, Turkey, and spans the time period 1938–1972 (Vorosmarty *et al.*, 1996). The end of the record in 1972 coincides with the initiation of the Greater Anatolia Project (GAP), a massive network of dams, hydroelectric power plants and irrigation projects, which marked the end of the publication of Turkish hydrological data (Kolars and Mitchell, 1991). A short record (1965–1972) of Tigris streamflow was measured at Baghdad, Iraq.

4.2. Methodology: spatial correlation

Correlations were calculated using temperature and precipitation records as a means of identifying those regions with the highest sensitivity to the NAO_{SLP} index (Plate 1(a)). Only stations having a record greater than or equal to 30 years and a complete winter (DJFM) record were selected. Table I lists the total number of temperature and precipitation stations after screening all records with less than 30 years of data and an incomplete winter (DJFM) season. Also shown is the number of stations containing at least 30, 40, 50, 60 and 70 years of temperature and precipitation data with the corresponding correlation coefficient indicating the 90%, 95% and 99% significance level. From this reduced dataset, containing 211 temperature and 403 precipitation stations, average winter temperature and precipitation were calculated, standardized and correlated against the Hurrell (1995) NAO_{SLP} index as a means of exploring linkages

Table I. Temperature and precipitation station data after screening procedure

	Temperature	Precipitation	$t_{90}\%$	$t_{95}\%$	$t_{99\%}$
n_{total}	770	591	—	—	—
$n>70$	79	192	0.195	0.232	0.302
$n>60$	95	245	0.211	0.250	0.325
$n>50$	113	277	0.231	0.273	0.354
$n>40$	142	323	0.257	0.304	0.393
$n>30$	211	403	0.295	0.349	0.449

Also listed is the number of stations containing at least 30, 40, 50, 60 and 70 years of temperature and precipitation data with the corresponding correlation coefficient indicating the 90%, 95% and 99% significance level.

between changes in North Atlantic surface ocean conditions and Middle Eastern climate. Plate 1(b and c) demonstrate spatial correlations between the NAO_{SLP} index and the mean winter (DJFM) temperature and precipitation for the circum-Atlantic and Mediterranean sectors.

4.3. Methodology: Turkish temperature and precipitation indices

Spatially integrated Turkish winter (DJFM) temperature and precipitation indices were constructed by first normalizing each temperature and precipitation station, and then averaging all temperature and precipitation records for the time period 1930–1995. The station-averaged time series was then correlated against the Hurrell (1995) NAO_{SLP} index.

For the temperature anomaly index, 23 Turkish stations (Figure 1) were first normalized (1930–1995 mean removed) and then averaged to produce a single composite index of Turkish winter temperature variability (°C). For the Turkish winter precipitation anomaly index, a total of 27 stations (Figure 1) were first normalized (1930–1995 mean removed) and then averaged to produce a single index of Turkish winter precipitation variability (mm/DJFM) spanning the same interval. Table II provides a listing of all Turkish stations (sorted by descending elevation) with respective record length, latitude, longitude and elevation. The correlation between Turkish temperature/precipitation indices and the NAO_{SLP} index (T_{r-val}, P_{r-val}), as well as the winter (DJFM) average temperature (T_{DJFM}) and precipitation (P_{DJFM}), are also presented.

Table II. Turkish stations used in temperature and precipitation indices

Station	n	lon°E	lat°N	Elev (m)	T_{r-val}	T_{DJFM} (°C)	P_{r-val}	P_{DJFM} (mm)
Kars	57	43.08	40.60	1775	—	—	0.32**	92.8
Erzurum	61	41.27	39.92	1756	0.45***	−5.84	0.51***	111.8
Van	40	43.32	38.45	1667	0.52***	−1.89	0.19	141.3
Sivas	61	37.02	39.75	1285	0.44***	−1.28	0.38**	164.6
Erzincan	40	39.50	39.73	1156	0.54***	−0.32	0.38*	124.6
Kayseri	40	35.48	38.78	1053	0.63***	1.02	0.41**	140.4
Afyon	40	30.53	38.75	1034	0.57***	2.32	0.50***	159.6
Konya	40	32.55	37.97	1032	0.61***	2.43	0.42***	137.6
Bursa	40	29.07	40.18	1001	0.38**	6.72	0.57***	322.6
Isparta	40	30.55	37.75	997	0.67***	3.49	0.68***	285.5
Ankara	60	32.90	40.00	894	0.37**	2.28	0.44***	156.7
Malatya	40	38.08	38.43	862	0.48**	2.40	0.27	178.8
Igdir	47	44.03	39.93	858	—	—	0.11	65.7
Kastamonu	40	33.77	41.37	799	0.50***	1.29	0.45**	120.2
Diyarbakir	60	40.18	37.88	686	0.47***	4.27	0.18	271.3
Mugla	40	28.35	37.20	646	0.52***	6.60	0.59***	771.8
Cankiri	38	33.60	40.60	630	—	—	0.47***	163.3
Urfa	40	38.77	37.13	547	0.42**	7.58**	—	—
Adana	61	35.42	37.00	73	0.34**	10.97	0.29*	387.4
Antalya	61	30.73	36.70	50	0.55***	11.07	0.34**	750.2
Edirne	61	26.57	41.67	48	—	—	0.64***	222.6
Istanbul	60	29.10	41.00	40	—	—	0.32***	319.7
Giresun	56	38.40	40.92	38	—	—	0.23	443.6
Kumkoy	40	29.00	41.30	30	—	—	0.27	346.9
Izmir	60	27.30	38.40	25	0.35**	9.52	0.44***	419.1
Samsun	68	36.33	41.28	4	0.44***	7.67	0.36**	251.9
Rize	60	40.50	41.00	4	0.49***	7.47	0.28*	820.4
Canakkale	40	26.40	40.13	3	0.38**	7.39	0.68***	329.6

* Denotes the 95% significance level (see text for further details).
** Denotes the 99% significance level (see text for further details).
*** Denotes the 99.9% significance level (see text for further details).
Record length (n); latitude (lat); longitude (lon) and elevation (elev).

5. RESULTS

The primary focus of this study is to establish and quantify the regional extent of the NAO and its impact on the Middle East. The following results demonstrate that interannual–decadal changes in Middle Eastern temperature, precipitation and Euphrates River streamflow are linked to coeval changes in North Atlantic climate.

5.1. Regional extent of NAO climate signatures

Global correlation analysis between the NAO_{SLP} index and the global station temperature (Plate 1(b)) and precipitation (Plate 1(c)) demonstrates the far-field influence of the NAO on Middle Eastern climate, and illustrates the distinct dipole relationship related to the subtropic–subpolar NAO pressure gradient. Plate 1(b) demonstrates that the Eastern Mediterranean temperature is negatively correlated with the NAO, whereas northern Europe is positively correlated with it. Much of the Mediterranean sector (stretching from the Iberian Peninsula to Italy) returns non-significant correlation values with respect to temperature. In Plate 1(c), the entire Mediterranean sector, extending from Portugal and Morocco through to Turkey, is negatively correlated with the NAO. The southeastern rim of the Mediterranean exhibits a positive correlation. All stations are shaded with respect to the 90%, 95% and 99% significance levels for 40 years of data, as listed in Table I. Stations which are not significantly correlated are not shaded.

During positive NAO years, Turkey becomes significantly cooler (Plate 1(b)) and drier (Plate 1(c)). The more zonal trajectories of Atlantic heat and moisture during negative NAO years bring anomalously warmer and wetter conditions to Turkey. This connection between the Middle East and the North Atlantic sector is evidently the easternmost limit of the NAO influence on Mediterranean climate, extending from Portugal and Morocco (Lamb and Peppler, 1987) to eastern Turkey. Correlations were also calculated for stations in Syria and Iraq (Table III). Northern Syria retains a significant NAO signal, albeit weaker than that in Turkey, whereas there is no significant correlation in Iraq. Lower winter (DJFM) rainfall correlations outside of Turkey reflect, in part, the characteristically low and highly variable rainfall pattern of the Middle East (Plate 1(c)).

5.2. The impact of the NAO in Turkey

In a study of the spatial and temporal variations of rainfall in Turkey, Turkes (1996a) noted that rainfall in the region is characterized by two major wet periods—1940–1948 and 1962–1970—and two major dry periods—1971–1974 and 1989–1993—with severe and widespread droughts occurring in 1973, 1984, 1989 and 1990. These periods, when compared with the NAO_{SLP} index shown in Figure 2(a), establish a connection between wet periods and a negative NAO, and drought periods and a positive NAO.

The resulting composite Turkish temperature and precipitation anomaly indices for the period 1930–1995 are significantly correlated with the NAO_{SLP} index. The Turkish temperature correlation r-value ($r = -0.42$, Figure 2(a)) indicates that 18% of the temperature variance is linearly related to the

Table III. Precipitation stations in Syria and Iraq with corresponding r-values (see text for further details)

Station	n	lon	lat	elev (m)	$P_{r\text{-}val}$
Damascus, Syria	35	36.52	33.32	610	−0.15
Kamishli, Syria	37	41.22	37.05	452	−0.26
Aleppo, Syria	39	37.22	36.18	390	−0.36**
Baghdad, Iraq	70	44.23	33.23	45	0.10

Record length (n); latitude (lat); longitude (lon) and elevation (elev).

NAO_{SLP} index. The Turkish precipitation correlation r-value ($r = -0.52$, Figure 2(b)) indicates that 27% of the Turkish winter precipitation variance is linearly related to the NAO_{SLP} index.

The Tigris and Euphrates River streamflow acts to integrate regional precipitation, thereby providing a spatially averaged time series of precipitation variability for stations located in the headwater region. Discharge data obtained from UNESCO (Vorosmarty *et al.*, 1996), measured at the headwater station Keban, in eastern Turkey (Figure 1; 38.48°N, 38.45°E), confirm that the 1938–1972 December–April (DJFMA) Euphrates streamflow time series is also highly correlated with the NAO_{SLP} index ($r = -0.42$, Figure 2(c)), with 18% of the variance linearly related to the NAO_{SLP}. A short, 8-year time series of Tigris streamflow measured at Baghdad, Iraq (Figure 1; 33.20°N, 44.30°E) follows the Euphrates streamflow variability from 1965 to 1972 (Figure 2(c)). All correlations exceed the 98% confidence level, and temperature and precipitation correlations exceed the 99.9% confidence level. The DJFMA interval was selected because it represents $\sim 50\%$ of the total annual streamflow and is representative of both precipitation and snowmelt, thereby combining temperature and precipitation variations.

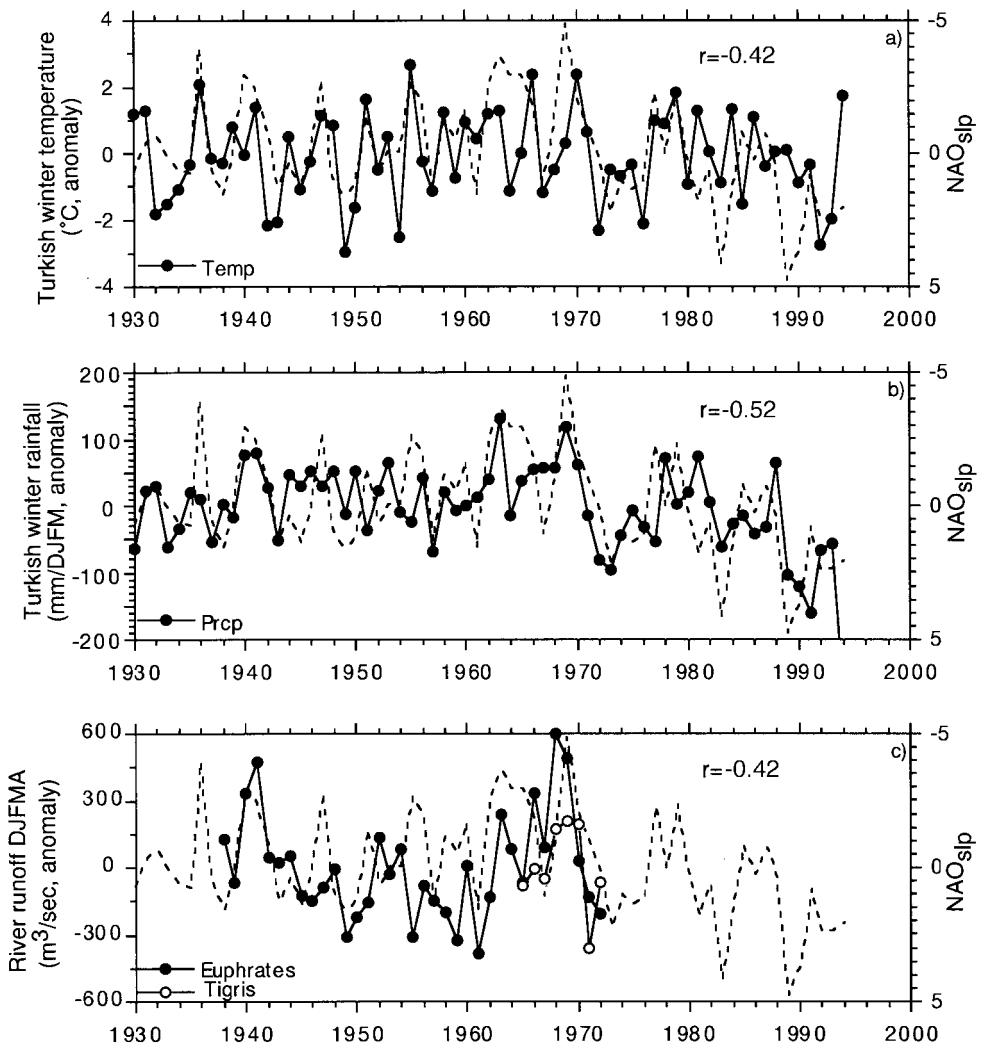

Figure 2. Correlation between the NAO_{SLP} index and (a) Turkish winter temperature index, (b) Turkish winter precipitation index and (c) DJFMA average streamflow of the Euphrates (filled circles) and the Tigris Rivers (open circles) (note: the NAO_{SLP} index has been multiplied by -1 for easier comparison)

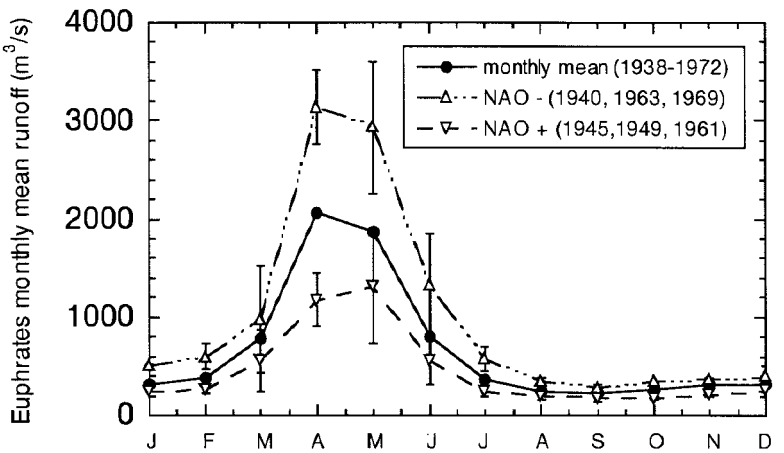

Figure 3. Monthly Euphrates River streamflow (solid line) measured at Keban, Turkey (35-year mean). Monthly averages for the three lowest NAO years (1940, 1963 and 1969; dashed line with filled circles, 2σ S.D. shown), and monthly averages of the three highest years (1945, 1949 and 1961; dashed line with triangles, 2σ S.D. shown)

The annual streamflow time series, measured from September–August, exhibits many of the same interdecadal trends evident in the NAO_{SLP} index, with low flow values during the 1950s and high flow values during the early 1940s and the late 1960s. The NAO influence on Euphrates streamflow is even more profound when NAO-extrema years are considered. The calculated average river runoff at Keban for the three highest (1945, 1949 and 1961; mean = 447 m^3/s) and the three lowest (1940, 1963 and 1969; mean = 983 m^3/s) NAO years demonstrates that the Euphrates streamflow exhibits $\sim \pm 40\%$ variability about the 35-year mean value (663 m^3/s) associated with NAO extrema (Figure 3).

5.3. Correlation with other indices

Previous studies have investigated links between Eastern Mediterranean climate and other large-scale climate phenomena (De Putter *et al.*, 1998; Price *et al.*, 1998; Kadioglu *et al.*, 1999). Price *et al.* (1998) examined the relationship between ENSO and precipitation in Israel and concluded that statistically significant correlations only appear in the last 25 years. As a follow-up to this study, Kadioglu *et al.* (1999) investigated variations in Turkish precipitation. Their results showed that changes associated with ENSO are primarily relegated to Southern Turkey, with variations on the order of $\pm 6\%$ of the monthly total precipitation value (Kadioglu *et al.*, 1999).

We also examined the possible influence of other large-scale climate phenomena on Middle Eastern climate. Correlations between our Turkish climate anomaly indices and indices of ENSO (NINO3 index) and the Asian monsoon intensity (All-India Rainfall index) were calculated. The Turkish temperature and precipitation indices are not significantly correlated with either NINO3 ($r = 0.20$ and 0.04, respectively) or Asian monsoon intensity ($r = 0.02$ and -0.12, respectively).

6. CONCLUSIONS

This study uses standard statistical techniques and a global archive of temperature and precipitation data to succinctly demonstrate the regional extent and the expected variability of measured physical parameters with respect to the NAO pressure dipole. A positive (negative) NAO dipole is the result of a strong (weak) meridional pressure gradient leading to a colder, dryer (warmer, wetter) Greenland/Mediterranean sector and a warmer, wetter (colder, dryer) northern Europe/northeast US/Scandinavia sector, as was first noted by Walker (1924). Results described in the paper provide evidence that the NAO is not limited to this classic dipole, but rather extends beyond the maritime north Atlantic and into the Middle East, a region

commonly neglected from North Atlantic study owing to its proximity to the monsoonal region and relatively sparse data coverage. The physical mechanism for this link is the secondary genesis of cyclonic storms, originating in the Atlantic, near to Crete, Cyprus and the Black Sea.

Investigations into NAO impacts have been extended to agricultural and fishery yields (Friedland *et al.*, 1997), as well as to African dust transport (Moulin *et al.*, 1997), demonstrating the increasingly important economic and political significance of this phenomenon. The impacts of the NAO are especially meaningful in light of recent episodes of drought in the Middle East, a region extremely sensitive to even the smallest changes in streamflow. Ongoing research efforts are aimed at understanding whether the NAO, like ENSO, is a coupled ocean–atmosphere phenomenon as opposed to a purely white noise time series. Coupled or ocean-only modes of variability are of interest because they have the potential to elevate predictability over a white noise (atmosphere)–red noise (ocean) system. Should the NAO prove to be predictable, future work should include long-range, early warning systems for drought/flood monitoring in the Middle East and the prediction of Turkish precipitation and streamflow.

Turkish temperature and precipitation time series show decreasing trends during the 1980s, which are consistent with the persistently positive NAO_{SLP} index during that time. We suggest that the Tigris–Euphrates streamflow time series would show this same decreasing trend, related solely to natural climate variability, if discharge information for this period was available. Calculation of the linear trend of Turkish temperature and precipitation anomaly indices shown in Figure 2(a and b) for the period 1982–1995 yields values of 1°C/decade and 82 cm/decade, significant at the 95% confidence limit. This precipitation trend is 26% of the 1930–1995 mean of 310/mm winter. Effective policy initiatives would be best served by incorporating both anthropogenic and natural variations in Tigris–Euphrates streamflow.

Increasing hydroelectric and agricultural demands on Tigris and Euphrates runoff, related to the $32 billion GAP, have exacerbated tense relations between the riparian neighbours and have led to claims of decreased water supply by Syria and Iraq. Turkey, because it has the good fortune of being situated at the headwaters of the Tigris–Euphrates River system, can literally turn off the water supply of its downstream neighbours and has threatened to do so on occasion (McCaffrey, 1993). For example, when the Ataturk Dam was completed in 1990, Turkey stopped the flow of the Euphrates entirely for 1 month, leaving Iraq and Syria in considerable distress. Similarly, in 1975, when the Syrians began filling Lake Assad after completion of work on the Tabqa Dam, Iraq threatened to bomb the dam, alleging that it seriously reduced the river's flow. Both countries amassed troops along the border. These military actions were in response to anthropogenic changes in water use imposed by one state against the others. Natural climate variability, however, which has no political alliances, affects water supply to this region as well and could easily be misinterpreted as anthropogenic.

ACKNOWLEDGEMENTS

We wish to thank Alexey Kaplan, Yochanan Kushnir, Balaji Rajagopolan and Rosanne D'Arrigo for their comments. This manuscript was prepared with AGU's LATEX macros v4, with the extension package 'AGU^{++}' by P.W. Daly, version 1.5c from 1997/03/14.

REFERENCES

Alpert P, Neeman B, Shay-ell Y. 1990. Climatological analysis of Mediterranean cyclones using ECMWF data. *Tellus* **18**: 65–67.

Baker C, Eischeid J, Karl T, Diaz H. 1995. The quality control of long-term climatological data using objective data analysis [preprints, AMS Ninth Conference on Applied Climatology, Dallas, TX, January 15–20]. Data accessed via the LDEO climate server http://ingrid.ldgo.columbia.edu/SOURCES/.NOAA/.NCDC/.GCPS/

Barnston A, Livezey R. 1987. Classification, seasonality and persistence of low-frequency atmospheric circulation patterns. *Monthly Weather Review* **115**: 1083–1126.

De Putter T, Loutre M, Wansard G. 1998. Decadal periodicities of Nile River historical discharge (ad 622–1470) and climatic implications. *Geophysical Research Letters* **25**(16): 3193–3196.

Friedland K, Reddin D, Kocok J. 1997. Marine survival of North American and European Atlantic salmon—effects of growth and environment. *ICES Journal of Marine Science* **50**: 481–492.

Gleick P. 1993. Water and conflict: fresh water resources and international security. *International Security* **18**: 79–112.

Henderson-Sellers A, Robinson PJ. 1992. *Contemporary Climatology*, (1st edn). John Wiley and Sons: New York.

Hillel D. 1994. *Rivers of Eden: The Struggle for Water and the Quest for Peace in the Middle East*, (1st edn). Oxford University Press: Oxford.
Hurrell J. 1995. Decadal trends in the North Atlantic Oscillation: regional temperatures and precipitation. *Science* **269**: 676–679.
Hurrell J. 1996. Influence of variations in extratropical wintertime teleconnections on Northern Hemisphere temperature. *Geophysical Research Letters* **23**: 665–668.
Hurrell J, Van Loon H. 1997. Decadal variations in climate associated with the North Atlantic Oscillation. *Climatic Change* **36**(3–4): 301–326.
Kadioglu M, Tulunay Y, Borhan Y. 1999. Variability of Turkish precipitation compared to El Niño events. *Geophysical Research Letters* **26**(11): 1597–1600.
Kinzer S. 1999. Where the Kurds seek a land, Turks want the water. *The New York Times* 28 February: 3.
Kolars J, Mitchell W. 1991. *The Euphrates River and the Southeast Anatolia Development Project*, (1st edn). Southern Illinois University Press: Carbondale.
Lamb P, Peppler R. 1987. North Atlantic Oscillation: concept and application. *Bulletin of the American Meteorological Society* **68**: 1218–1225.
McCaffrey S. 1993. Water, politics, and international law. In *Water in Crisis*, Gleick P (ed.). Oxford University Press: New York, 92–99.
Moulin C, Lambert C, Dulac F, Dayan U. 1997. Control of atmospheric export of dust from North Africa by the North Atlantic Oscillation. *Nature* **387**: 691–694.
Price C, Stone L, Huppert A, Rajagopalan B, Alpert P. 1998. A possible link between El Niño and precipitation in Israel. *Geophysical Research Letters* **25**(21): 3963–3966.
Rogers JC, van Loon H. 1979. The seesaw in winter temperatures between Greenland and northern Europe. Part ii: some oceanic and atmospheric effects in middle and high latitudes. *Monthly Weather Review* **107**: 509–519.
Rogers, JC. 1984. The association between the North Atlantic Oscillation and the Southern Oscillation in the Northern Hemisphere. *Monthly Weather Review* **112**: 1999–2015.
Saabye H. 1942. Brudstykker sd en Dagbog holden I Grönland I Aarene 1770–1778. In *Medd. Grönland*, 45, 103, Oesterman H. (ed.).
Shapland G. 1997. *Rivers of Discord: International Water Disputes of the Middle East*, 1st edn. St. Martin's Press: New York.
Turkes M. 1996a. Meteorological drought in Turkey: a historical perspective 1930–1993. *Drought Network News* **8**: 17–21.
Turkes M. 1996b. Spatial and temporal analysis of annual rainfall variations in Turkey. *International Journal of Climatology* **16**: 1057–1076.
van Loon H, Rogers JC. 1978. The seesaw in winter temperatures between Greenland and northern Europe. Part I: winter. *Monthly Weather Review* **104**: 365–380.
Vorosmarty B, Fekete B, Tucker B. 1996. Global river discharge data (rivdis v1.0), Technical Report. UNESCO.
Walker GT. 1924. Correlations in seasonal variations of weather. IX. *Memoirs Indian Meteorology Department* **24**: 275–332.
Walker G, Bliss E. 1932. World weather V. *Memoirs of the Royal Meteorological Society* **4**: 53–84.

